Solid-State Electronics 197 (2022) 108442

Contents lists available at ScienceDirect

Solid State Electronics

journal homepage: www.elsevier.com/locate/sse

Theoretically probing the relationship between barrier length and resistance in Al/AlO$_x$/Al tunnel junctions☆

Paul Lapham, Vihar Georgiev *

Device Modelling Group, James Watt School of Engineering, University of Glasgow, Glasgow G12 8QQ, United Kingdom

ARTICLE INFO

Keywords:
DFTB
NEGF
Josephson Junctions
Material modeling
Electron tunneling

ABSTRACT

Al/AlO$_x$/Al tunnel junctions, also known as Josephson Junctions, are key components of many established and emerging electronic devices. They are an essential component of superconducting qubits. A major drawback is a lack of understanding of how the amorphous AlO$_x$ barrier influences the electron transport properties. In this work we combined Tight Binding Density Functional Theory (DFTB) with Non Equilibrium Greens Function (NEGF) to study computationally several Al/AlO$_x$/Al with different barrier lengths. The simulations reveal a weak exponential relationship between barrier length and resistance of the device. However, considerable variability is found between junctions of similar barrier length. The calculations provide evidence of an "effective" barrier length significantly smaller than the actual (physical) barrier length. The resistance and effective barrier is found to be sensitively influenced by the local atomic structure of the amorphous barrier, which explains the junction to junction variability.

1. Introduction

One of the most popular qubit architectures is the superconducting qubit, which relies on the physics of the Josephson Junction (JJ) [1]. One of the main challenges faced in quantum computing systems is decoherence time of each qubit, which is often linked to two level defects within the JJ structure [2]. JJs are tri-layer systems that consist of two superconductors separated by a thin insulating barrier, typically Al/AlO$_x$/Al. The thin oxide barrier is amorphous which is considered one of the main causes for noise and decoherence in qubit circuits [3]. There is still a poor understanding from an atomic perspective of how the structure of the amorphous oxide affects performance and subsequent failures in qubit applications.

There are many different variables within JJs structure that can sensitively influence qubit's stability and performance [4]. Barrier length is considered a key junction parameter, with typical barrier lengths ranging between 1–2 nm. However, the physical barrier length is difficult to determine and control. It has been shown that the effective barrier length can be orders of magnitude smaller than the physical (actual) barrier length [5]. Thus, it is critical to understand the nature of transport through the barrier. The current flow between Al under an applied drain bias consists of electron tunneling through the thin insulating barrier. In this work we combine Tight Binding Density Functional methods (DFTB) and Non-Equilibrium Greens Function (NEGF) for an efficient method to probe theoretically the influence of the barrier length and atomic structure on the electron transport of Al/AlO$_x$/Al tunnel barriers.

The main aim is to understand, from an atomistic level and prospective, how electron transport is affected by the atomic structure of the amorphous barrier. Through our simulation, we can explore the existence of an "effective barrier length" over a physical one and understand what structural effects lead to the reduction of this parameter.

2. Simulation methodology

All calculations were carried out using the QuantumATK-2021 software [6]. The electronic properties of the Al/AlO$_x$/Al tunnel junctions were simulated with DFTB using the "matsci-0-3" parameter set [7,8]. Although a semi-empirical method parameterized for certain systems with DFT, it has been shown to be transferable and suggests it can describe the important physics of the systems with reasonable accuracy whilst significantly reducing the computational cost [9]. The electron transport properties of the junction were studied using non-equilibrium Green's function (NEGF), a powerful tool for a three-dimensional, atomistic treatment of transport. The amorphous oxide barrier was built by simulated annealing method using Molecular Dynamics as described several times in the literature using the "ReaxFF" force field [10]. The final device model is periodic in x and y with open boundary conditions in the transport direction, z. A Monkhorst–Pack grid k-point sampling

☆ The review of this paper was arranged by Francisco Gamiz.

* Corresponding author.
E-mail address: vihar.georgiev@glasgow.ac.uk (V. Georgiev).

https://doi.org/10.1016/j.sse.2022.108442

Available online 30 August 2022

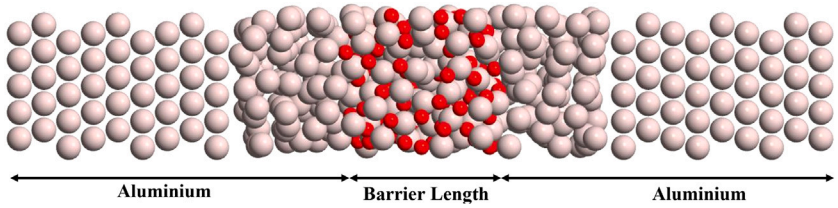

Fig. 1. Illustration of a model Al/AlO_x/Al Junction studied in this work. Grey-Aluminum, Red-Oxygen. (For interpretation of the references to color in this figure legend, the reader is referred to the web version of this article.)

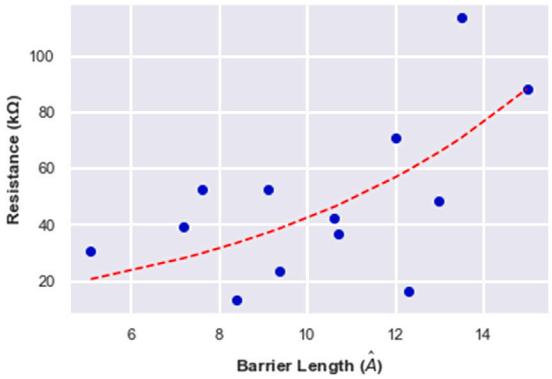

Fig. 2. Computed Resistance vs Barrier Length. The red line is an exponential fit to guide the eye. (For interpretation of the references to color in this figure legend, the reader is referred to the web version of this article.)

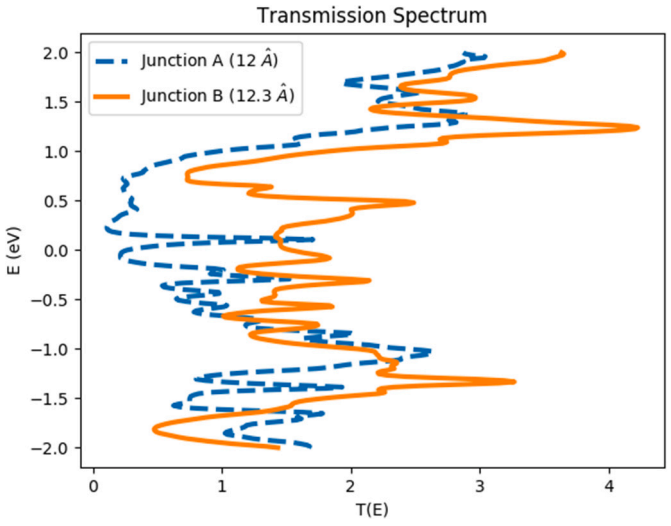

Fig. 3. Computed Transmission Spectra for two Junctions with similar barrier length.

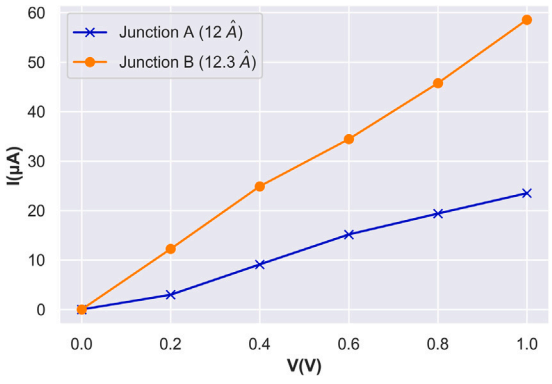

Fig. 4. Computed I-V Curves for Junction A and Junction B.

of 5 × 5 × 300 was used in the transport calculations whilst a 9 x 9 sampling was used to resolve the transmission.

Key to theoretically exploring the transport of the aluminum oxide tunnel junctions with NEGF is the calculation of the Transmission probability given by

$$T(\epsilon) = Tr[G(\epsilon)\Gamma^{L}(\epsilon)G^{\dagger}(\epsilon)\Gamma^{R}(\epsilon)] \tag{1}$$

Where $G(\epsilon)$ is the retarded Green's function and $\Gamma^{L/R}$ is the broadening functions in terms of the self-energies. Full details of the NEGF method can be found in the literature [11–13].

From the transmission probability, using the Landauer–Buttiker formalism, where current is computed as:

$$I = \frac{2e^2}{h}\int T(\epsilon)[f_L(\epsilon) - f_R(\epsilon)]d\epsilon \tag{2}$$

where $f_{L/R}$ are the Fermi functions of the electrodes [13].

Normal state resistance is a key junction parameter, as it can be related to the critical current of the tunnel junction when superconducting, through the Ambegaokar–Baratoff equation [14]. The resistance of the model junctions are calculated first by calculating the zero bias conductance of the system:

$$G = -\frac{2e^2}{h}\int T(\epsilon)\frac{\delta f_0(\epsilon)}{\delta\epsilon}d\epsilon \tag{3}$$

where f_0 is the equilibrium Fermi–Dirac distribution function, the resistance can then be estimated from the inverse of conductance:

$$R_N = \frac{1}{G} \tag{4}$$

3. Results and discussion

For accurate modeling of the Al/AlO_x/Al it is key to ensure an amorphous oxide barrier. This is generated through Molecular Dynamics (MD) simulated annealing method as previously described in the literature [15]. The amorphous barrier is then placed between bulk aluminum electrodes and relaxed using DFTB geometry optimization to approximate the Al-AlO_x interface. This method is repeated for different oxide barrier lengths in order to explore the influence of the barrier length on the junction transport properties. An example model of the junctions studied in this work is shown in Fig. 1. The final device is studied by combining DFTB and NEGF methods to explore the electron transport (tunneling current) in the device in normal operation (i.e not superconducting conditions). The computed resistance from 13 different junctions are shown in Fig. 2. It is expected that the relationship between barrier length and resistance is exponential, with increasing barrier length the resistance increases. As can be seen from Fig. 2 the relationship is not straightforward. A slight exponential relationship can be seen as guided by the red-dashed line. However, there is considerable variability in resistance values for junctions with similar barrier lengths. This is clearly seen at ≈ 12 Å, the junctions have a similar barrier length but differ in resistance by a factor of 4. Work carried out by Dorneles et al. showed that in some Al/AlO_x/Al junctions the effective tunneling area was significantly smaller than the actual area of the device [5]. Furthermore, this indicates a different "effective barrier length" compared to the physical one. The results of our simulations could be explained by the existence of an effective

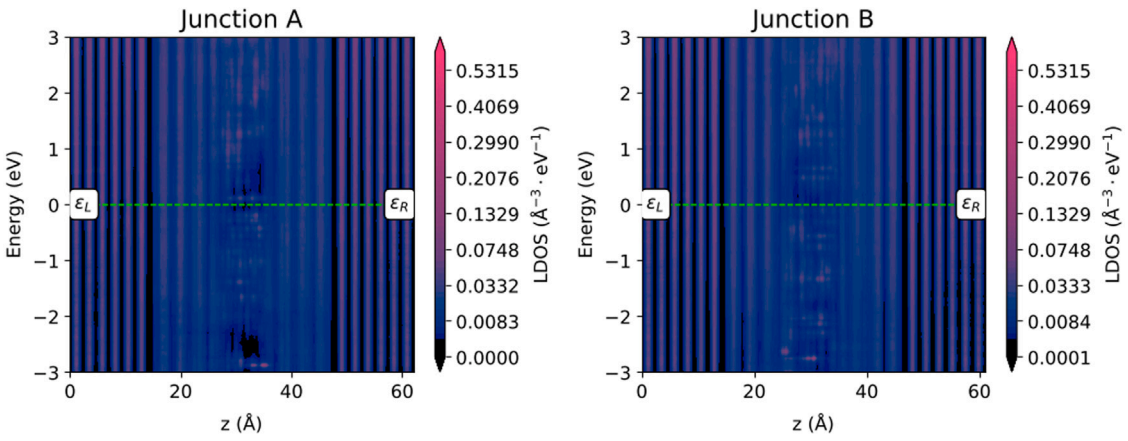

Fig. 5. PLDOS for Junction A and B which provides an insight to the different electronic structure of the barriers.

barrier length. Hence, significant variability in Resistance (R) for junctions with similar measured barrier length arises due to considerably different effective tunneling area due to the local atomic structure in the barrier.

To further explore how the nature of the amorphous barrier influences the tunneling probability and hence the current flow which leads to significant variability in resistance, the rest of this paper focuses on two junctions (A and B) with similar physical barrier lengths (12 and 12.3 Â) which differ considerably in normal state resistance (70.8 and 16.5 kΩ). The predicted Transmission spectra for these two junctions is shown in Fig. 3.

Fig. 3 shows that the transmission of these two junctions vary considerably (despite peaks at similar energies), hence the difference in resistance. Despite very similar barrier length, stoichiometry and density, the inherent differences in disorder of the amorphous barriers leads to different effective tunneling pathways and subsequently different effective barrier length. This is highlighted when comparing the Transmission spectra of these two junctions and thus the resistance of the barriers.

The Current–Voltage (I–V) characteristics for both junctions were computed between an applied drain bias of 0-1 V. This is shown in Fig. 4. The IV Curves are consistent with the respective resistances. Junction B (which has lower resistance) is predicted to have a considerably higher current than that for Junction A. This clearly highlights the sensitivity of the transport to the atomic structure of the amorphous barrier. Although the barrier length only differs by 0.3 Angstroms, the effective area of the barrier which is responsible for the tunneling current must be considerably different for these two junctions.

Further analysis of the electronic structure of the two junctions reveals how the local atomic structure of the amorphous barrier sensitively influences the transport properties. The Projected Local Density of States (PLDOS), shown in Fig. 5, help explain the predicted resistances of the junctions. Small gaps in DOS around the Fermi level ('pinholes') are evident for Junction A. This break in DOS leads to a break in conduction pathways, increasing the resistance of the junction. As this is projected on the local atomic structure, it clearly shows how the differences in local structure and disorder of the amorphous AlO_x has a significant effect on the junction transport.

Fig. 6 shows the transmission pathways at the Fermi level for both Junction A and Junction B. Analysis of transmission pathways is a key advantage of our atomistic approach. It illustrates, there are dominant atoms in an area of the amorphous barrier responsible for electron transport. Here, an insight can be gained on why the resistance varies considerably despite similar barrier length, stoichiometry,

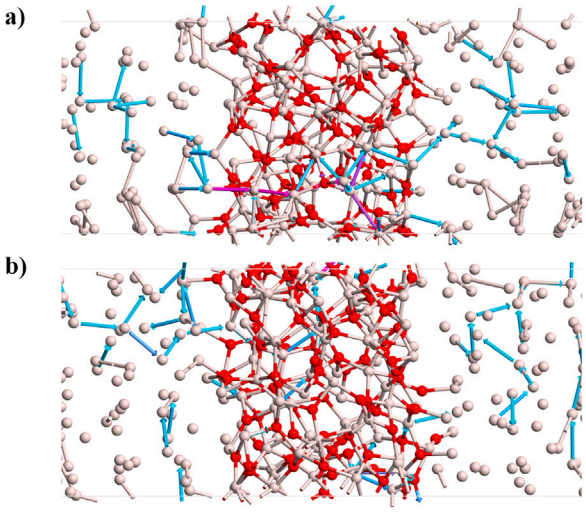

Fig. 6. (a) Transmission Pathways at Fermi level for Junction A (b) Transmission Pathways at Fermi level for B, illustrating considerable differences in tunneling despite similar barrier length.

density. Breaking down the local bond contributions to the T(E) at specific energies (Fermi-energy in Fig. 6) shows that Metal–Metal bonds have the highest contribution, indicative of "metallic hotspots" in the barrier. This finding is consistent with previous reports in the literature [10,15]. When inspecting the Transmission pathways at different energy, there are always common atoms responsible for all transmission, highlighting the "hot spots" and effective tunneling area hypothesis.

Understanding how the amorphous barrier influences the transport of the model junctions and real junctions is critical for improving device to device variability and reducing two level defects in the systems. Improving this is key to several applications of the $Al/AlO_x/Al$ tunnel barriers. Evidence of an effective tunnel barrier, smaller than a physical one, is significant for understanding variability. The challenge is two-fold, quantifying this barrier and understanding what structural characteristics lead to the effective barrier. One hypothesis is the structural order and positioning of oxygen throughout the barrier. The more oxide in the barrier the larger the resistance, therefore it would be sensible to suggest that the local arrangement of oxide will be key to the resistance of the device. As the barriers are amorphous this can differ significantly.

The transmission pathways show a concentration of metal–metal pathways. By computing the electron density map of the structure, as

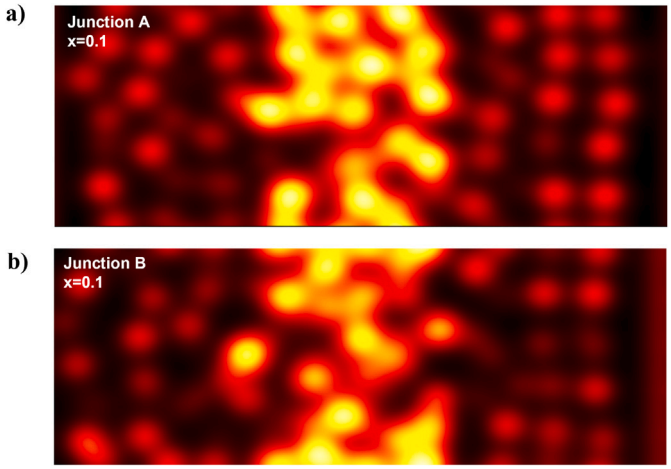

Fig. 7. Electron Density map of (a) Junction A and (b) Junction B. This 2-D xy cutplane was taken at 0.1*X-direction of the device. The yellow "hotspots" are concentrated at regions of high oxygen concentration. (For interpretation of the references to color in this figure legend, the reader is referred to the web version of this article.)

in Fig. 7, the picture becomes clearer. The intense yellow heat-map shows the concentration of electron density around the oxygen. From this particular cut, it can be seen a more intense heat-map for Junction A than B, with more "gaps" through the barrier for Junction B. This is further evidence of how the local structure sensitively affects tunneling probability (and so resistance). Although only one cut plane of electron density for each junction is reported here for brevity, similar pattern is evident across the entire device in both cases.

4. Conclusion

This work has combined DFTB and NEGF atomistic methods to study a wide range of model Al/AlO_x/Al tunnel junctions with different amorphous AlO_x barrier lengths. An insight has been gained into the relationship between the barrier length and the resistance of the device, a key parameter for understanding the superconducting critical currents of the junction.

The simulations show a weak exponential relationship between barrier length and resistance, whilst a wide variability across the junctions is observed. This wide variability is evidence of how the local structure of the barrier sensitively affects the transport. Furthermore, the simulations provide further evidence for the existence of an effective tunneling barrier which is significantly smaller than the physical one. This helps explain the unexpected variability. Further work will focus on understanding what characteristics of the structure of the barrier controls the resistance. In addition, quantifying the effective barrier/tunneling area is currently being explored.

Declaration of competing interest

The authors declare the following financial interests/personal relationships which may be considered as potential competing interests: Paul Lapham reports financial support was provided by Engineering and Physical Sciences Research Council (EP/P009972/1). Vihar Georgiev reports financial support was provided by Quantum Computng and Simulaton ub Partnership Resource Fund.

Data availability

Data will be made available on request.

References

[1] Kjaergaard M, Schwartz ME, Braumüller J, Krantz P, Wang JI, Gustavsson S, et al. Superconducting qubits: Current state of play. Annu Rev Condens Matter Phys 2020;11:369–95. http://dx.doi.org/10.1146/annurev-conmatphys-031119-050605, arXiv:1905.13641.

[2] Müller C, Cole JH, Lisenfeld J. Towards understanding two-level-systems in amorphous solids: Insights from quantum circuits. Rep Progr Phys 2019;82(12). http://dx.doi.org/10.1088/1361-6633/ab3a7e, arXiv:1705.01108.

[3] Zeng L, Tran DT, Tai CW, Svensson G, Olsson E. Atomic structure and oxygen deficiency of the ultrathin aluminium oxide barrier in Al/AlOx/Al Josephson junctions. Sci Rep 2016;6(March):1–8. http://dx.doi.org/10.1038/srep29679.

[4] Kim CE, Ray KG, Lordi V. A density-functional theory study of the Al/AlOx/Al tunnel junction. J Appl Phys 2020;128(15). http://dx.doi.org/10.1063/5.0020292.

[5] Dorneles LS, Schaefer DM, Carara M, Schelp LF. The use of simmons' equation to quantify the insulating barrier parameters in Al/AlOx/Al tunnel junctions. Appl Phys Lett 2003;82(17):2832–4. http://dx.doi.org/10.1063/1.1569986.

[6] Smidstrup S, Markussen T, Vancraeyveld P, Wellendorff J, Schneider J, Gunst T, et al. Quantumatk: An integrated platform of electronic and atomic-scale modelling tools. J Phys Condens Matter 2020;32(1). http://dx.doi.org/10.1088/1361-648X/ab4007, arXiv:1905.02794.

[7] Frenzel J, Oliveira AF, Duarte HA, Heine T, Seifert G. Structural and electronic properties of bulk gibbsite and gibbsite surfaces. Zeitschrift Fur Anorg Und Allg Chemie 2005;631(6–7):1267–71. http://dx.doi.org/10.1002/zaac.200500051.

[8] Guimarães L, Enyashin AN, Frenzel J, Heine T, Duarte HA, Seifert G. Imogolite nanotubes: Stability, electronic, and mechanical properties, vol. 1, no. 4. 2007.

[9] Spiegelman F, Tarrat N, Cuny J, Dontot L, Posenitskiy E, Martí C, et al. Density-functional tight-binding: basic concepts and applications to molecules and clusters. Adv Phys X 2020;5(1). http://dx.doi.org/10.1080/23746149.2019.1710252.

[10] Cyster MJ, Smith JS, Vaitkus JA, Vogt N, Russo SP, Cole JH. The effect of atomic structure on the electrical response of aluminium oxide tunnel junctions. Phys Rev 2019;013110:1–10. http://dx.doi.org/10.1103/physrevresearch.2.013110, arXiv:1905.12214.

[11] Maassen J, Harb M, Michaud-Rioux V, Zhu Y, Guo H. Quantum transport modeling from first principles. Proc IEEE 2013;101(2):518–30. http://dx.doi.org/10.1109/JPROC.2012.2197810.

[12] O'Donnell R. Modeling of nanoscale devices. Proc IEEE 2008;96(9):1509–10. http://dx.doi.org/10.1109/JPROC.2008.927311.

[13] Datta S. Quantum Transport: Atom to Transistor. New York: Cambridge Univ. Press; 2005.

[14] Ambegaokar V, Baratoff A. Tunneling between superconductors. Phys Rev Lett 1963;10:486–9. http://dx.doi.org/10.1103/PhysRevLett.10.486, URL https://link.aps.org/doi/10.1103/PhysRevLett.10.486.

[15] Lapham P, Georgiev V. Computational study of oxide stoichiometry and variability in the Al/AlOx/Al tunnel junction. Nanotechnology 2022. http://dx.doi.org/10.1088/1361-6528/ac5f2e.